Universe Scientific Publishing

DOI:10.18686/ahe.v7i14.8656

Characterization of Defects in Perovskite Thin Film Materials Using Microscopic Techniques

Yanan Zhang, Guangliang Yao, Jie Chu

Taishan University, Tai'an 271021, PR China

Abstract: In recent years many efforts have been made to figure out the underlying photophysical mechanisms operated in the perovskite-based devices. Observing and understanding these defects through experimental characterization methods is a necessary step to obtain high-performance perovskite. Herein, we attempt to systematically summarize the defect determination techniques based on microscopy from the scale of single perovskite layer, emphasizing the representative mechanisms of microscopy in explaining the defects.

Keywords: Material defects; Microtechnology; Perovskite thin film

Fund Project:

This work was supported by the National Nature Science Foundation of China (No.: 52102290), Tai'an Science and Technology Development Plan (2021GX0075) and School enterprise cooperation project (2022HX103).

1. Introduction

As is known to us all, perovskite materials show promising photovoltaic properties including broad absorption spectrum with high absorption coefficient, fast carrier mobility, long carrier diffusion lengths and low-cost fabrication processing.[1, 2] Despite of this, the persuit of more efficient and stable PSCs is still facing tough bottleneck on the way of industrialization, most of which are related with the lattice defects and trap states resulting from the polycrystalline and ionic nature of perovskite materials.

In the most common precursor solution preparation of metal halide perovskite films, it is inevitable to produce inherent imperfections in the lattice, which are usually element lost or structural disorder formed during the crystallization dynamic equilibrium of fast solvent evaporation and annealing process.[3, 4] What is more, there are various kinds of intrinsic defects in perovskite lattice like point defects in the bulk and at the and surfaces, including vacancies, interstitials and anti-site occupations.[5, 6] For example, regardless of the difference in formation energy, the point defects that may appear in $MAPbI_3$ films are MA, Pb and I vacancies, MA, Pb and I interstitials, and MA_{Pb}, MA_I, Pb_{MA}, Pb_I, I_{MA} and I_{Pb} anti-site occupations.[7] It has been reported that among all kinds of crystal defects in both organic-inorganic hybrid perovskites and all-inorganic perovskites, undercoordinated lead ion (Pb^{2+}) is in the majority because of its relatively lower formation energy.[8] Pinhole, microcrack, precipitates and impurities are also easily observed in perovskite films, leading to poor contact with the transport layer and increasing series resistance of the final photovoltaic device. On the other hand, the appropriate underlying substrate plays a prerequisite role in the crystallization of perovskite film, whose thermal expansion coefficients need to match each other.[9, 10] Otherwise, the lattice strain and subsequent defects can be created in the top perovskite film, reducing the film quality and causing energy loss.[11]

It is paramount to eliminate the complex trap states for the broader applications of perovskite-based devices. Defect passivation means converting the deep-level defects into the shallow-level defects, greatly suppressing nonradiative recombination in devices.[10] It is urgent and necessary to understand the in-depth mechanism and extent qualitatively as well as quantitatively, especially about the passivation effects on the entire photovoltaic processes from the carrier generation, transport to extraction. Unfortunately, it is difficult to realize this determination by a single state-of-art technique. Even the bridge connecting the crystal defects and the optoelectronic properties of perovskites still lack direct experimental characterization. Commonly, the pristine and passivated perovskite films are

compared with the help of microscopy- and spectroscopy-based methods which provide significant variation of charge carrier dynamics and recombination. For instance, microscopy techniques offer visualized surface coverage of the polycrystalline perovskite film, to examine the variation of recombination process in the single perovskite layer.

In this review, multiple experimental techniques that have been carried out to characterize the undesirable defects in the perovskite layer are systematically discussed. Surface morphology, crystal structure properties of perovskite films are determined, which are followed by well-established schemes linking those phenomena with defects rightfully.

2. Microscopy-based Techniques for Defect Characterizations

The surface morphologies of perovskite films can be demonstrated by microscopy-based technologies with different fields of view, which directly image the grain defects and relevant features.

2.1 SEM

For the polycrystalline perovskite films, the morphology plays a key role in optoelectronic quality. SEM images provide the information of surface coverage, grain size and grain boundary. It has been widely recognized that high-performance perovskite films need to meet the requipment of smooth, uniform and dense morphological features with few pinholes or voids. The mainstream belief among most research groups is that growing perovskite film with large grain size will lower the amount of defects and improve the phase stability.[12] In other words, large perovskite grain can avoid the recombination centers that are sufficiently present at grain boundaries and benefit efficient transport of charge carriers, which mitigates the loss of voltage fundamentally.[13, 14] Chen and colleagues reported that the introduced BA^+ governed the colloidal size and nucleation sites, thus producing smooth RP perovskite films with enlarged grain size and optimized crystal preferential orientation and obviously reduced trap states. [15] The introduction of a second space cation including PEA^+, PMA^+, and iso-BA^+ into $BA_2MA_{n-1}Pb_nI_{3n+1}$ contributed to the enlarged grain size of over 1 μm (Figure 9a,b) and the optimized crystal growth orientation, significantly enhancing the device performance. This contribution has been attributed to the aggregation in the precursor solution induced by the second space cation, which decreased the nucleation sites and finally enlarged the crystal grains.[16] Moreover, the ion migration which easily occurs thorough grain boundaries in perovskite films was found to be suppressed, consequently limiting the hysteretic phenomenon and performance degradation of PSCs.[17, 18] The ceaseless pursuit of enlarging grain size in perovskite film has been encouraging a great number of fabrication methods to control the nucleation and growth processes and achieving grain size varying from nanometer to micrometer. However, as a matter of fact, Muscarella et al. demonstrated that oriented large grains of methylammoinium lead iodide ($MAPbI_3$) perovskite did not exhibit longer charge carrier lifetime or higher carrier mobility than those of film with smaller grain size, which meant that differences in grain size would not affect optoelectronic properties as the crystallographic grains were usually misidentified in SEM images.[19]

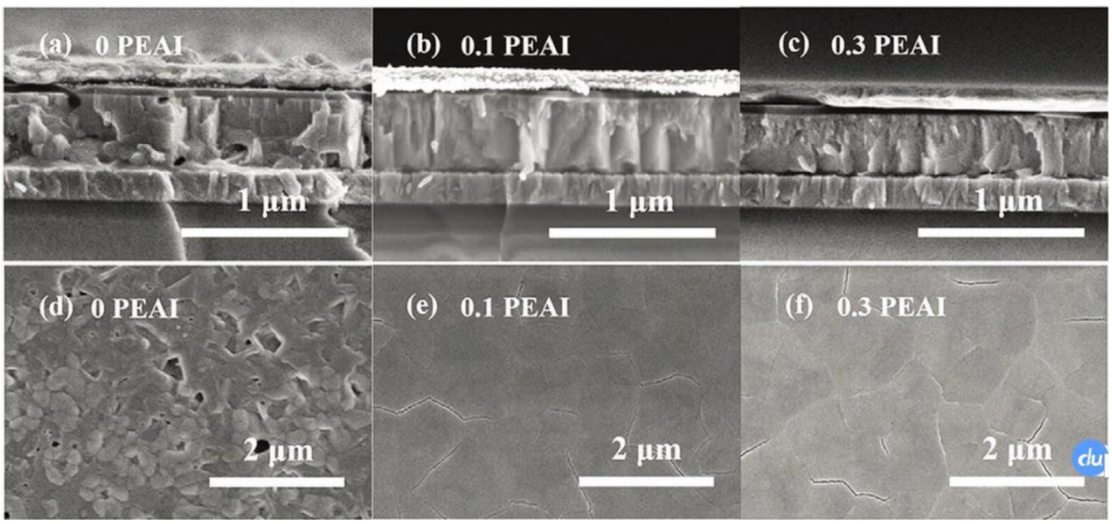

Figure 1. a-c) Cross-sectional SEM images, e-f) top-view SEM images of $BA_2MA_4Pb_5I_{16}$ perovskite films with different amounts of PEA^+ as a second space cation. [16]

2. 2 AFM

As one of the typical microscopy-based techniques, the atomic force microscopy (AFM) is applied to map the surface morphology, thickness and roughness of perovskite films in sub-nanometer resolution. Three-dimensional (3D) and two-dimensional (2D) topographical images of surfaces provided by AFM cover a great characterization range from 500 nm to 50 μm, what is larger than that of SEM measurement. Generally speaking, compact perovskite film with full coverage and homogeneous grain size distribution

is desirable. On the other hand, apart from the detection of particle size and surface coverage which is similar to the above-mentioned SEM, AFM demonstrates arithmetic roughness (Ra) root mean square roughness by the probe tip contacting with the perovskite material directly. Since the highly rough surface with inhomogeneous grain size may be responsible for disappointing interface contact and adverse effect on charge transport, low roughness is often demanded for the final device performance.[20] This can indicate the presence, density and distribution of defects to some extent.

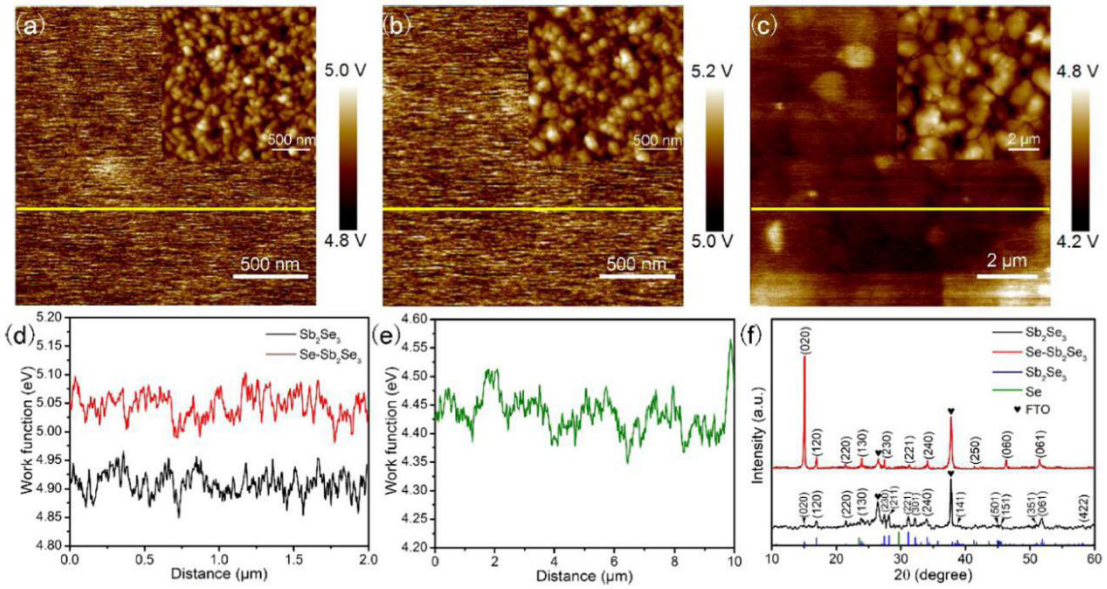

Figure 2. KPFM images and the corresponding AFM images (insets) of (a) Sb_2Se_3, (b) Se-Sb_2Se_3, and (c) $CsPbBrI_2$ films. Corresponding surface potential profiles of (d) Sb_2Se_3, Se-Sb_2Se_3, and (e) $CsPbBrI_2$ films. (f) XRD patterns of Sb_2Se_3 films with and without selenization.[22]

There are many variant modes of AFM with the help of additional accessories, of which the Kelvin probe force microscopy (KPFM) offers the chemical potential of perovskite film relative to that of the substrate.[21] Potential topography maps of Sb_2Se_3, Se-Sb_2Se_3, and the perovskite films are shown in Figure 2a-c with the corresponding atomic force microscopy (AFM) images inserted. The surface morphologies of the Sb_2Se_3 and Se-Sb_2Se_3 films are uniform, with no impurity phase observed. There are obvious holes and relatively sharp crystals in the Sb_2Se_3 film without selenization, in contrast to the Se-Sb_2Se_3 film, which is much smoother and denser. As a consequence of calibrating the cantilever on the reference Au sample, the work function of each film along the line is given directly in Figure 2d, e. It can be seen that the work functions of Sb_2Se_3 and Se-Sb_2Se_3 are around 4.91 and 5.05 eV, respectively, whereas that of $CsPbBrI_2$ is approximately 4.43 eV. Namely, the Fermi level (EF) of Sb_2Se_3 lies a little shallower than that of Se-Sb_2Se_3, probably suggesting a heaver p-type nature of Se-Sb_2Se_3. The crystallization information of Sb_2Se_3 and Se-Sb_2Se_3 films is demonstrated by the X-ray diffraction (XRD) patterns in Figure 2f. The stronger intensities of the diffraction peaks for Se-Sb_2Se_3 compared with Sb_2Se_3 imply that the Se-Sb_2Se_3 film is highly crystallized. [22] When the cantilever calibrated on the reference Au, KPFM can also directly determine the work function (absolute Fermi level) and further confirm the position of the conduction band. Combined with the data derived from the ultraviolet-visible (UV-Vis) spectrophotometry, the determination of valence band can be realized.[23]

2.3 TEM

TEM is one of the most commonly used techniques for the nano-structural defect feature study of semiconductors, providing detection of both bulk and surface defects thanks to the penetration depth of the electron beam.[24] Equipped with additional accessories, TEM can be carried out to identify the crystallography and element distribution. The former function relies on selected area electron diffraction (SAED) which is capable of phase detection, while the later one comes from energy dispersive spectrometer (EDS). However, the microscopic morphology as well as the chemical and structural analysis of the hot perovskite materials by TEM did not go well, since both organic-inorganic hybrid perovskites and all-inorganic perovskites are not stable enough under the intense electron beam in high-resolution model. Once the beam intensity rises up to the atomic-resolution level, rapid structural degradation occurs, hindering accurate investigation of the original perovskites. Some researchers proposed the idea of cryogenic electron microscopy, where the perovskite samples are examined in low temperature environment with low-dose intensity to reduce electron-beam damage. [25]

Cryogenic electron microscopy is carried out for probing both structural and chemical information in inaccessible length scale

of atomic resolution. Thanks to fast freezing cryogens, cryo-transfer protocols and measured at liquid nitrogen temperature, fragile samples are protected from side reactions and electron beam damage, maintaining in their native states.[26] Li et al. compared the TEM images for $MAPbI_3$ hybrid perovskite that were obtained from standard and cryogenic TEM methods.[27] A short exposure to ambient conditions when transferred and inserted into the TEM column as well as the unavoidable sublimation of volatile organic components under high vacuum could induce unwanted side reactions of $MAPbI_3$ nanowire (NW) sample, leading to clear surface structural degradation into PbI_2. On the contrary, the cryogenic protocol including cryogenic sample loading and low-dose imaging with plunge-freezing endowed atomically resolved interrogation without clear degradation, offering $[PbI_6]^{4-}$ octahedral of the hybrid perovskite in pristine state.

2.4 STM

As another powerful tool for structure characterization at the atomic scale, scanning tunneling microscopy (STM) has been applied in the surface morphology analysis and interfacial structure investigation of perovskites as well. Surface defects and molecular compounds of perovskite film can be examined, together with crystallographic arrangements in atomic resolution.[28] With the aim to get insight into the local density of states in the surface of perovskite film, STM need to be performed in an inert atmosphere or vacuum condition to avoid exposure to humidity and air.[29, 30] In Figure 3, the decrease of tunneling conductance is observed in the passivated film compared with the control one, which is indicative of reduced density of defect states and low recombination velocity.[23]

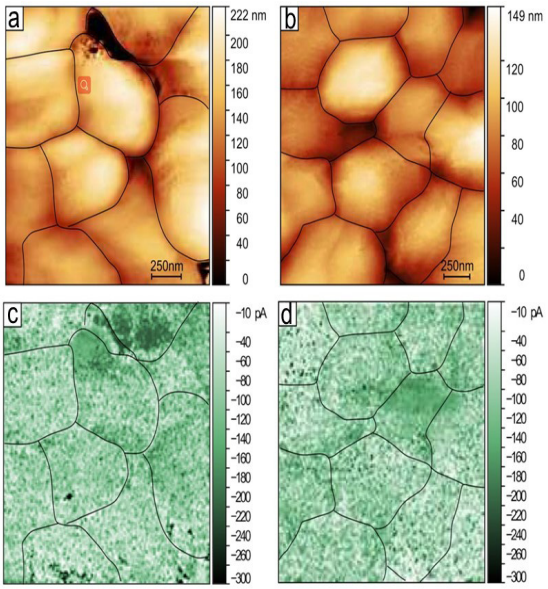

Figure 3. STM images of a) the control sample and b) the target sample. c, d) are their constant current imaging spectroscopies at -2V respectively.[23]

3. Summary

In conclusion, we comprehensively summarized multiple microscopies utilized to test defect characterization of on the scale of perovskite thin films. All these above methods highlight the importance of testing environment and point to the relationships between the chemistry, structure and property. How the defects appear, move and interact with other components remains mystery. The development of determination techniques performed in situ and/or in operation will indeed stimulate the path towards viable PSCs with high performance, expediting the commercial applications in the near future.

References:

[1] J.-P. Correa-Baena, M. Saliba, T. Buonassisi, M. Grätzel, A. Abate, W. Tress, A. Hagfeldt, Science, 2017, 358, 739.

[2] R. Verduci, A. Agresti, V. Romano, G. D'Angelo, Materials, 2021, 14, 5843.

[3] Q. A. Akkerman, G. Rainò, M. V. Kovalenko, L. Manna, Nature materials, 2018, 17, 394.

[4] Z.-J. Yong, S.-Q. Guo, J.-P. Ma, J.-Y. Zhang, Z.-Y. Li, Y.-M. Chen, B.-B. Zhang, Y. Zhou, J. Shu , J.-L. Gu, Journal of the American Chemical Society, 2018, 140, 9942.

[5] F. Gao, Y. Zhao, X. Zhang , J. You, Advanced Energy Materials, 2020, 10, 1902650.
[6] Z. Ni, C. Bao, Y. Liu, Q. Jiang, W.-Q. Wu, S. Chen, X. Dai, B. Chen, B. Hartweg, Z. Yu, Science, 2020, 367, 1352.
[7] J. M. Ball, A. Petrozza, Nature Energy, 2016, 1, 1.
[8] L. Fu, H. Li, L. Wang, R. Yin, B. Li, L. Yin, Energy & Environmental Science, 2020, 13, 4017.
[9] K. B. Lohmann, J. B. Patel, M. U. Rothmann, C. Q. Xia, R. D. Oliver, L. M. Herz, H. J. Snaith, M. B. Johnston, ACS Energy Letters, 2020, 5, 710.
[10] D. Luo, W. Yang, Z. Wang, A. Sadhanala, Q. Hu, R. Su, R. Shivanna, G. F. Trindade, J. F. Watts, Z. Xu, Science, 2018, 360, 1442.
[11] T. A. Doherty, A. J. Winchester, S. Macpherson, D. N. Johnstone, V. Pareek, E. M. Tennyson, S. Kosar, F. U. Kosasih, M. Anaya, M. Abdi-Jalebi, Nature, 2020, 580, 360.
[12] Z. Xiao, Q. Dong, C. Bi, Y. Shao, Y. Yuan, J. Huang, Advanced Materials, 2014, 26, 6503.
[13] H. D. Kim, H. Ohkita, H. Benten, S. Ito, Advanced Materials, 2016, 28, 917.
[14] A. Sharenko, M. F. Toney, Journal of the American Chemical Society, 2016, 138, 463.
[15] S. Chen, N. Shen, L. Zhang, L. Zhang, S. H. Cheung, S. Chen, S. K. So, B. Xu, Adv. Funct. Mater. 2020, 30, 1907759.
[16] X. Lian, J. Chen, M. Qin, Y. Zhang, S. Tian, X. Lu, G. Wu, H. Chen, Angew. Chem., Int. Ed. 2019, 58, 9409.
[17] T. Niu, J. Lu, R. Munir, J. Li, D. Barrit, X. Zhang, H. Hu, Z. Yang, A. Amassian, K. Zhao, Advanced Materials, 2018, 30, 1706576.
[18] P. Liu, N. Han, W. Wang, R. Ran, W. Zhou, Z. Shao, Advanced Materials, 2021, 33, 2002582.
[19] L. A. Muscarella, E. M. Hutter, S. Sanchez, C. D. Dieleman, T. J. Savenije, A. Hagfeldt, M. Saliba, B. Ehrler, The Journal of Physical Chemistry Letters, 2019, 10, 6010.
[20] L. Fu, Y. Nie, B. Li, N. Li, B. Cao, L. Yin, Solar RRL, 2019, 3, 1900233.
[21] H. Arandiyan, S. S. Mofarah, C. C. Sorrell, E. Doustkhah, B. Sajjadi, D. Hao, Y. Wang, H. Sun, B.-J. Ni, M. Rezaei, Chemical Society Reviews, 2021, 50, 10116.
[22] L. Fu, B. Li, L. Yin, ACS Applied Energy Materials, 2020, 3, 9550.
[23] A. Krishna, H. Zhang, Z. Zhou, T. Gallet, M. Dankl, O. Ouellette, F. T. Eickemeyer, F. Fu, S. Sanchez, M. Mensi, Energy & Environmental Science, 2021, 14, 5552.
[24] E. J. Jang, J. Lee, J. H. Kwak, Catalysis Today, 2020, 352, 323.
[25] D. Zhang, Y. Zhu, L. Liu, X. Ying, C.-E. Hsiung, R. Sougrat, K. Li, Y. Han, Science, 2018, 359, 675.
[26] Z. Zhang, Y. Cui, R. Vila, Y. Li, W. Zhang, W. Zhou, W. Chiu, Y. Cui, Accounts of Chemical Research, 2021, 54, 3505.
[27] Y. Li, W. Zhou, Y. Li, W. Huang, Z. Zhang, G. Chen, H. Wang, G.-H. Wu, N. Rolston, R. Vila, Joule, 2019, 3, 2854.
[28] Y. Tison, H. Lin, J. Lagoute, V. Repain, C. Chacon, Y. Girard, S. Rousset, L. Henrard, B. Zheng, T. Susi, ACS Nano, 2013, 7, 7219.
[29]Y . Fu, M. T. Rea, J. Chen, D. J. Morrow, M. P. Hautzinger, Y. Zhao, D. Pan, L. H. Manger, J. C. Wright, R. H. Goldsmith, Chemistry of Materials, 2017, 29, 8385.
[30] S. Yang, S. Chen, E. Mosconi, Y. Fang, X. Xiao, C. Wang, Y. Zhou, Z. Yu, J. Zhao, Y. Gao, Science, 2019, 365, 473.